TOOTH CONTACT ANALYSIS OF NOVIKOV CONVEXO-CONCAVE GEARS

Tadeusz Markowski, Michał Batsch

S u m m a r y

Paper presents mathematical model of convexo-concave Novikov gear mesh. The parametric equations of teeth surface and units normal were obtained. Based on condition of continuous tangency of teeth surfaces, the tooth contact analysis for both ideal gears and real ones was given. Thesis presents also the method for obtaining contact pattern, on the basis of which a number of computer simulations were carried out, aiming at examining the influence of chosen gear parameters on its contact region. The presented results simulation of meshing will be used to design the Novikov gears, which will be made and tested on the circulating power test machine.

Keywords: tooth contact analysis, Novikov gears, contact pattern

Analiza styku zębów przekładni wklęsło-wypukłych typu Nowikowa

S t r e s z c z e n i e

Opracowano matematyczny model wklęsło-wypukłego zazębienia typu Nowikowa. Określono parametryczne równania powierzchni bocznych zębów oraz równania wersorów normalnych do tych powierzchni. Przeprowadzono analizę styku zębów dla przekładni idealnej i rzeczywistej z uwzględnieniem warunku ciągłej styczności powierzchni bocznych zębów. Przedstawiono metodę wyznaczania obszaru styku, z wykorzystaniem której wykonano symulacje komputerowe. Celem symulacji jest ustalenie wpływu wybranych parametrów przekładni na jej ślad styku. Analiza wyników symulacji współpracy zębów stanowi podstawę do zaprojektowania przekładni Nowikowa. Przekładnia będzie wykonana i poddana próbie na stanowisku mocy krążącej.

Słowa kluczowe: analiza styku zębów, koła zębate Nowikowa, ślad styku

1. Introduction

Modern gearboxes should be characterized by high efficiency, low noise levels and high load capacity at as small dimensions as possible. A common teeth profile in gear transmissions is an involute one, where a convex pinion tooth flank works with a convex wheel tooth flank. The character of this work is particularly adverse in case of surface strength. If the increase of the surface load capacity is required it is necessary to increase the radius of tooth profiles and therefore pitch diameter or pressure angle. Pressure angle can be increased by

Address: Prof. Tadeusz MARKOWSKI, Michał BATSCH, MSc, Eng., Rzeszow University of Technology, Department of Mechanical Engineering, 8 Powstańców Warszawy Ave., 35-959 Rzeszów, corresponding author: e-mail: mbatsch@prz.edu.pl, tmarkow@prz.edu.pl

means of correction. Further increase of surface strength is connected with increasing the overall dimension of a gearbox.

Due to the above-mentioned disadvantage of the involute teeth profile there were attempts to withdraw from it. The alternative could be gear transmissions with convexo-concave teeth profiles. One of these profiles is Novikov tooth profile, in which circular arcs appear in a transverse section. This kind of gearing was applied in the final reduction stage of Westland Lynx helicopter gearbox (Fig. 1) [1, 2].
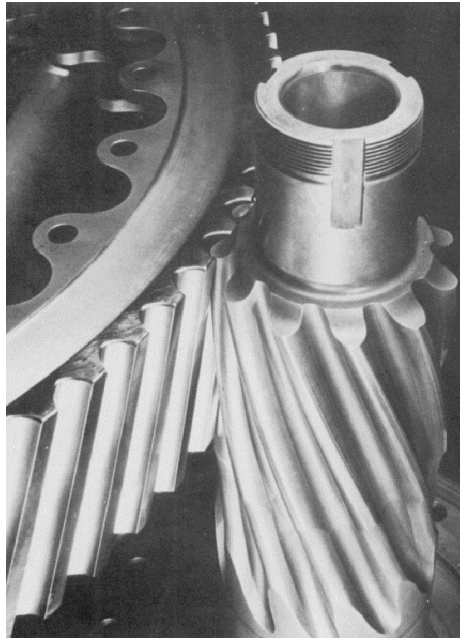

Fig. 1. Novikov gears manufactured
in Westlands-Helicopters ltd., based on [1]

The pinion has convex teeth whereas the wheel has the concave ones. The gearbox was a reducer of reduction ratio 20. The convexo-concave teeth profile allowed to decrease the number of gears to 40% of number of involute gears used previously [3].

The aim of this work is to develop the methods of tooth contact analysis [4] and investigating the influence of gear parameters on a contact region. The achieved results will be used to design the optimal parameters and modification of teeth of gearbox which will be tested. What's more the presented mathematical model of gear mesh can be used to simulate the milling process [5] of such kind of gears.

2. Geometric model of gear mesh

The analysed gearbox is a parallel helical gear pair consists of two Novikov gears with one line of action. A pinion has a convex tooth profile whereas a wheel has concave one which is shown in Fig. 2.
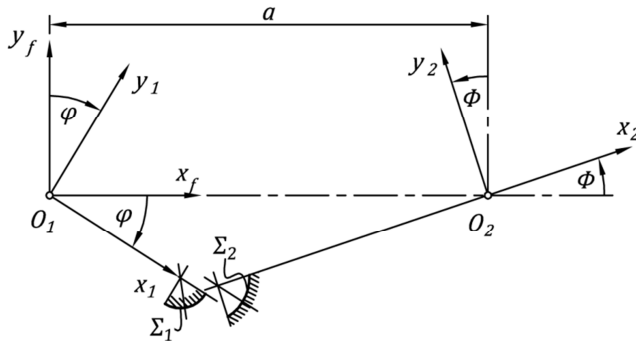

Fig. 2. Geometric model of Novikov gear mesh

The stationary coordinate system f connected with a wheel case as well as coordinate systems connected with pinion 1 and wheel 2 were established. Pinion rotates clockwise about z_1-axis which passes through point O_1 by the angle φ. The wheel rotates counterclockwise about z_2-axis which passes through point O_2 by the angle Φ. The distance between centers a is also the distance between the centers of coordinate systems. The surface of pinion Σ_1 in coordinate system 1 is represented by a position vector $\overline{r}_1^{(1)}$ and unit normal $\overline{n}_1^{(1)}$. Similarly, the surface of wheel Σ_2 in coordinate system 2 is represented by position vector $\overline{r}_2^{(2)}$ and unit normal $\overline{n}_2^{(2)}$. Surfaces of pinion and wheel teeth with their units normal are represented in coordinate system f by equations (1) and (2):

$$\overline{r}_1^{(f)} = M_{f1}\, \overline{r}_1^{(1)} \tag{1}$$

$$\overline{r}_2^{(f)} = M_{f2}\, \overline{r}_2^{(2)} \tag{2}$$

where: M_{f1} is the homogeneous matrix of transformation from 1 to f, M_{f2} is the homogeneous matrix of transformation from 2 to f. If the gear position errors (Fig. 3) should be taken into consideration the coordinate system 2 must be

translate through the x_f, y_f, z_f – axes about Δa_x Δa_y and Δa_z, and rotate about a constant x_f, y_f – axes respective by the angles κ_x i κ_y.

Elastic deformations of shafts	
Elastic deformations of bearings	
Bearing slackness	
Displacement from manufacturing and assembly errors	
Elastic deformations of wheel case	

1 - nominal position of axis 1
2 - nominal position of axis 2
3 - real position of axis 2
f_x - non-parallelism of gears axes
f_y - misalignment of gears axes
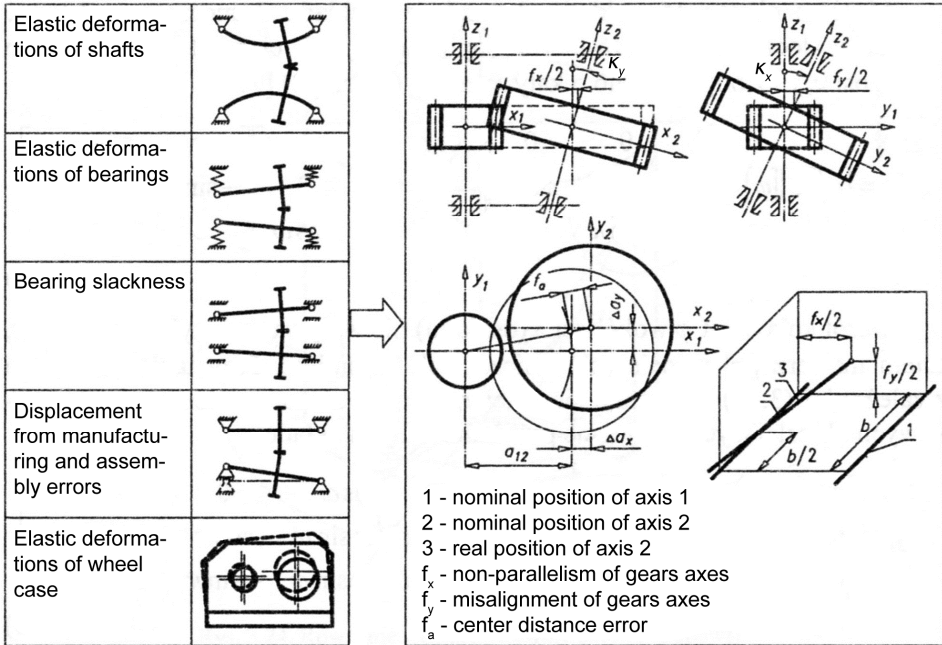f_a - center distance error

Fig. 3. Gear position errors, based on [6]

In this purpose the auxiliary coordinate system h was established (Fig. 4).
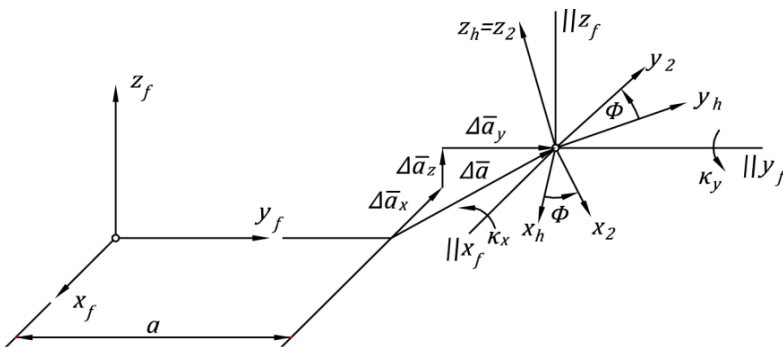

Fig. 4. Position and orientation of auxiliary coordinate system h

After taking into account the gear position errors the wheel will be rotating about new translated and misaligned $z_h = z_2$ – axis. According to the Fig. 4, matrix of transformation is given by formula (3)

$$M_{f2} = M_{fh}M_{h2} \tag{3}$$

where: M_{hf} is the homogeneous matrix of transformation from h to f, M_{h2} is the homogeneous matrix of transformation from 2 to h. Each matrices will be given as:

$$M_{f1} = \begin{bmatrix} \cos\varphi & \sin\varphi & 0 & 0 \\ -\sin\varphi & \cos\varphi & 0 & 0 \\ 0 & 0 & 1 & 0 \\ 0 & 0 & 0 & 1 \end{bmatrix} \tag{4}$$

$$M_{h2} = \begin{bmatrix} \cos\phi & -\sin\phi & 0 & 0 \\ \sin\phi & \cos\phi & 0 & 0 \\ 0 & 0 & 1 & 0 \\ 0 & 0 & 0 & 1 \end{bmatrix} \tag{5}$$

$$M_{fh} = \begin{bmatrix} \cos\kappa_y & \sin\kappa_x \sin\kappa_y & \cos\kappa_x \sin\kappa_y & \Delta a_x \\ 0 & \cos\kappa_y & -\sin\kappa_x & \Delta a_y \\ \sin\kappa_y & \sin\kappa_x \cos\kappa_y & \cos\kappa_x \cos\kappa_y & a + \Delta a_z \\ 0 & 0 & 0 & 1 \end{bmatrix} \tag{6}$$

The units normal of the surfaces in coordinate system f are expressed by formulas:

$$\bar{n}_1^{(f)} = L_{f1}\bar{n}_1^{(1)} \tag{7}$$

$$\bar{n}_2^{(f)} = L_{f2}\bar{n}_2^{(2)} \tag{8}$$

where: L_{f1} is the matrix of transformation from 1 to f, L_{f2} is the matrix of transformation from 2 to f. The above-mentioned transformation matrices can be obtained by crossing out the last row and the last column of the homogeneous matrices of transformation.

Figure 5 presents a transverse cross-section of Novikov gear pair.

The pinion with convex teeth and pitch radius r_1 is mated with the wheel with concave teeth and pitch radius r_2. The contact point of teeth profiles B is defined by the transverse pressure angle α_w. The O' point is the center of convex tooth profile with radius ρ_1, whereas the O point is the center of concave tooth profile with radius ρ_2. The C point is the contact point of pitch circles and is called the central point of meshing.
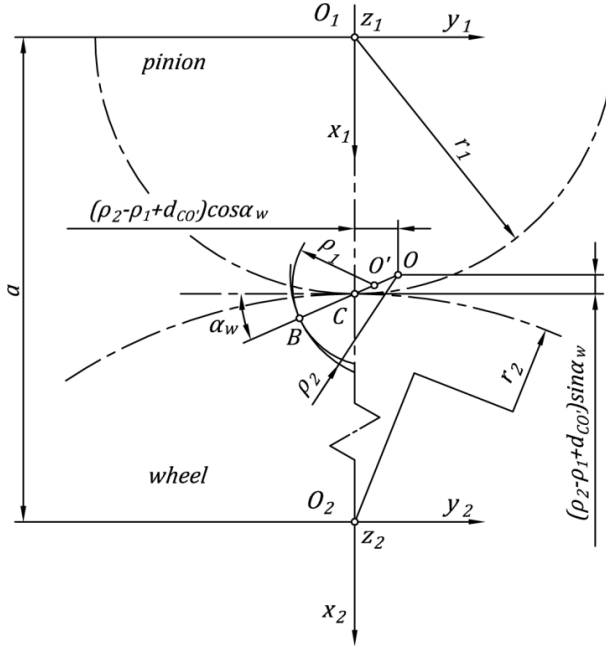
Fig. 5. Transverse section of working Novikov gears: α_w – transverse pressure angle, r_1 – pinion pitch radius, r_2 – wheel pitch radius, ρ_1 – convex teeth profile radii, ρ_2 – concave teeth profile radii, a – distance between axes, $d_{CO'}$ – distance between central point of meshing C and center of convex tooth profile O'

Teeth profiles in pinion and wheel coordinate systems are expressed by parametric equations (9) and (10)

$$\begin{cases} x_1 = \rho_1\cos\theta_1 + r_1 - d_{CO'}\sin\alpha_w \\ y_1 = \rho_1\sin\theta_1 + d_{CO'}\cos\alpha_w \end{cases} \tag{9}$$

$$\begin{cases} x_2 = \rho_2\cos\theta_2 - r_2 - (\rho_2 - \rho_1 + d_{CO'})\sin\alpha_w \\ y_2 = \rho_2\sin\theta_2 + (\rho_2 - \rho_1 + d_{CO'})\cos\alpha_w \end{cases} \tag{10}$$

Parametric equation of surface of convex tooth was obtained by a simultaneous rotation and translation of circular arc (9). Generating of pinion tooth surface is shown in Fig. 6.
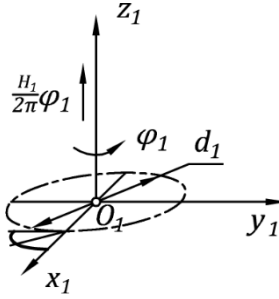
Fig. 6. Pinion tooth surface generating

The vector representation of pinion tooth surface is therefore given by (11)

$$
\bar{r}_1^{(1)} = \begin{bmatrix} r_{x1}^{(1)} \\ r_{y1}^{(1)} \\ r_{z1}^{(1)} \\ 0 \end{bmatrix} = \begin{bmatrix} \cos\varphi_1 & -\sin\varphi_1 & 0 & 0 \\ \sin\varphi_1 & \cos\varphi_1 & 0 & 0 \\ 0 & 0 & 0 & \dfrac{H_1}{2\pi}\varphi_1 \\ 0 & 0 & 0 & 1 \end{bmatrix}
$$
$$
\cdot \begin{bmatrix} \rho_1\cos\theta_1 + r_1 - d_{CO'}\sin\alpha_w \\ \rho_1\sin\theta_1 + d_{CO'}\cos\alpha_w \\ 0 \\ 1 \end{bmatrix} \tag{11}
$$

where: φ_1 is the screw line parameter, θ_1 is the circle parameter, H_1 is the lead of the screw line which is given by (12)

$$
H_1 = \frac{2\pi r_1}{tg\beta} \tag{12}
$$

where β is helix angle on the pitch cylinder. Finally after the substitution of (12) in (11) the surface of pinion tooth is expressed by formula (13)

$$
\bar{r}_1^{(1)} = \begin{bmatrix} \rho_1\cos(\theta_1 + \varphi_1) + r_1\cos\varphi_1 - d_{CO'}\sin(\alpha_w + \varphi_1) \\ \rho_1\sin(\theta_1 + \varphi_1) + r_1\sin\varphi_1 + d_{CO'}\cos(\alpha_w + \varphi_1) \\ \varphi_1 r_1 ctg\beta \\ 1 \end{bmatrix} \tag{13}
$$

Similarly the parametric equation of surface of concave tooth was obtained by a simultaneous rotation and translation of circular arc (10). Generating of wheel tooth surface is shown in Fig. 7.
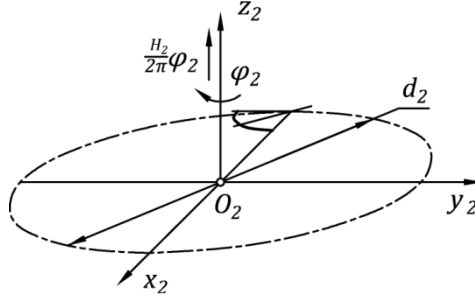
Fig. 7. Wheel tooth surface generating

The vector representation of wheel tooth surface is therefore given by (14)

$$\bar{r}_2^{(2)} = \begin{bmatrix} r_{x2}^{(2)} \\ r_{y2}^{(2)} \\ r_{z2}^{(2)} \\ 0 \end{bmatrix} =$$

$$= \begin{bmatrix} \cos\varphi_2 & \sin\varphi_2 & 0 & 0 \\ -\sin\varphi_2 & \cos\varphi_2 & 0 & 0 \\ 0 & 0 & 0 & \dfrac{H_2}{2\pi}\varphi_2 \\ 0 & 0 & 0 & 1 \end{bmatrix} \begin{bmatrix} \rho_2\cos\theta_2 - r_2 - (\rho_2 - \rho_1 + d_{CO'})\sin\alpha_w \\ \rho_2\sin\theta_2 + (\rho_2 - \rho_1 + d_{CO'})\cos\alpha_w \\ 0 \\ 1 \end{bmatrix} \tag{14}$$

where: φ_2 is the screw line parameter, θ_2 is the circle parameter, H_2 is the lead of the screw line which is given by (15)

$$H_2 = \frac{2\pi r_2}{\text{tg}\beta} \tag{15}$$

Finally after the substitution of (15) in (14) the surface of wheel tooth is expressed by formula (16)

$$\bar{r}_2^{(2)} = \begin{bmatrix} \rho_2\cos(\theta_2 - \varphi_2) - r_2\cos\varphi_2 - (\rho_2 - \rho_1 + d_{CO'})\sin(\alpha_w - \varphi_2) \\ \rho_2\sin(\theta_2 - \varphi_2) + r_2\sin\varphi_2 + (\rho_2 - \rho_1 + d_{CO'})\cos(\alpha_w - \varphi_2) \\ \varphi_2 r_2\text{ctg}\beta \\ 1 \end{bmatrix} \tag{16}$$

The units normal of the surfaces of tooth of pinion and wheel in coordinate systems respective *1* and *2* are given by equations (17) and (18)

$$\bar{n}_1^{(1)} = \begin{bmatrix} n_{x1}^{(1)} \\ n_{y1}^{(1)} \\ n_{z1}^{(1)} \end{bmatrix} = \frac{\dfrac{\partial r_1^{(1)}}{\partial \varphi_1} \times \dfrac{\partial r_1^{(1)}}{\partial \theta_2}}{\left| \dfrac{\partial r_1^{(1)}}{\partial \varphi_1} \times \dfrac{\partial r_1^{(1)}}{\partial \theta_2} \right|} = \begin{bmatrix} \dfrac{-\text{ctg}\beta\cos(\theta_1 + \varphi_1)}{\sqrt{\text{ctg}^2\beta + \sin^2\theta_1}} \\ \dfrac{-\text{ctg}\beta\,\sin(\theta_1 + \varphi_1)}{\sqrt{\text{ctg}^2\beta + \sin^2\theta_1}} \\ \dfrac{\sin\theta_1}{\sqrt{\text{ctg}^2\beta + \sin^2\theta_1}} \end{bmatrix} \tag{17}$$

$$\bar{n}_2^{(2)} = \begin{bmatrix} n_{x2}^{(2)} \\ n_{y2}^{(2)} \\ n_{z2}^{(2)} \end{bmatrix} = \frac{\dfrac{\partial r_2^{(2)}}{\partial \theta_2} \times \dfrac{\partial r_2^{(2)}}{\partial \varphi_2}}{\left| \dfrac{\partial r_2^{(2)}}{\partial \theta_2} \times \dfrac{\partial r_2^{(2)}}{\partial \varphi_2} \right|} =$$
$$= \begin{bmatrix} \dfrac{r_2\text{ctg}\beta\cos(\theta_2 - \varphi_2)}{\sqrt{r_2^2\text{ctg}^2\beta + \left(r_2\sin\theta_2 + (\rho_2 - \rho_1 + d_{CO\prime})\cos(\theta_2 - \propto_w)\right)^2}} \\ \dfrac{r_2\text{ctg}\beta\sin(\theta_2 - \varphi_2)}{\sqrt{r_2^2\text{ctg}^2\beta + \left(r_2\sin\theta_2 + (\rho_2 - \rho_1 + d_{CO\prime})\cos(\theta_2 - \propto_w)\right)^2}} \\ \dfrac{-(\rho_2 - \rho_1 + d_{CO\prime})\cos(\theta_2 - \propto_w) + r_2\sin\theta_2}{\sqrt{r_2^2\text{ctg}^2\beta + \left(r_2\sin\theta_2 + (\rho_2 - \rho_1 + d_{CO\prime})\cos(\theta_2 - \propto_w)\right)^2}} \end{bmatrix} \tag{18}$$

3. Condition of continuous tangency

The condition of continuous tangency expresses in a system of equations (19) [7, 8].

$$\begin{cases} \bar{r}_1^{(f)}(\varphi_1, \theta_1, \varphi) = \bar{r}_2^{(f)}(\varphi_2, \theta_2, \phi) \\ \bar{n}_1^{(f)}(\varphi_1, \theta_1, \varphi) = \bar{n}_2^{(f)}(\varphi_2, \theta_2, \phi) \end{cases} \tag{19}$$

The first equation of the system ensures that teeth surfaces have common point. The second equation of the system ensures the continuous tangency of surfaces. The goal of a tooth contact analysis is to solve this system of equations. It can be done numerically for each discrete value of angle of rotation of pinion.

As a result the relationships between surface parameters, the angle of rotation of wheel and the angle of rotation of pinion (20) can be found.

$$\varphi_1(\varphi), \theta_1(\varphi), \varphi_2(\varphi), \theta_2(\varphi), \phi(\varphi) \tag{20}$$

The substitution of functions (20) in parametric representation of teeth surfaces (13), (16) and (3.1), (3.2) gives the line of contact and the locus of contact points on teeth surfaces (Fig. 8).
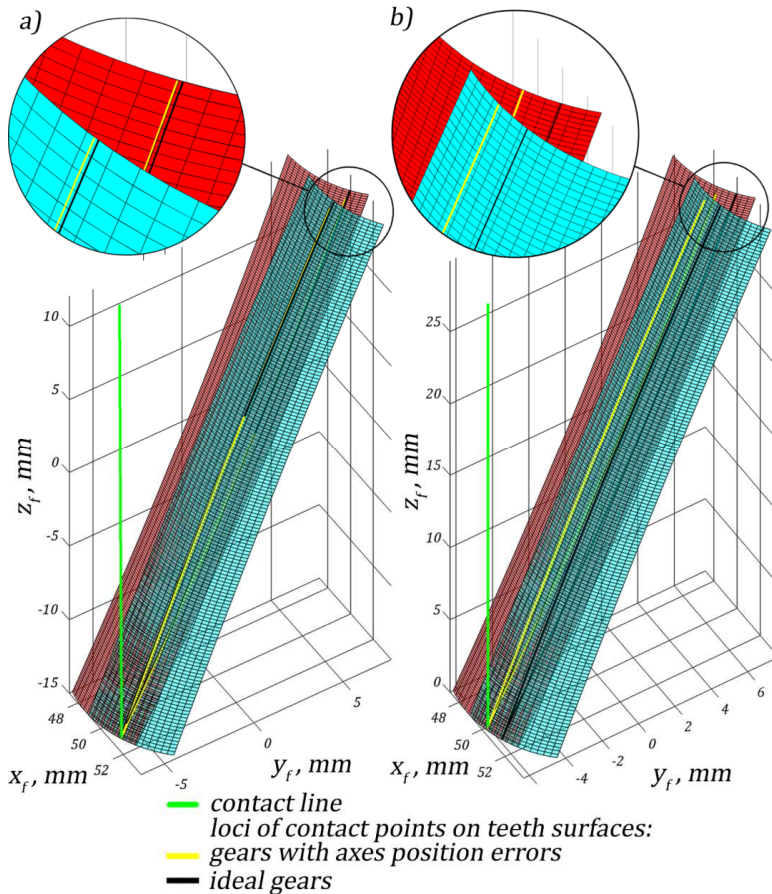

Fig. 8. Contact lines and loci of contact points on teeth surfaces: a) gears with axes misaligned error, b) gears with axes distance error

In case of ideal gear pair without axes position errors contact line is a straight line parallel to the z_f-axis which passes through B point. That means that the contact point moves through the gear width while rotating the gears.

The loci of contact points on teeth surfaces of pinion and wheel are the parts of helix which lies on the φ_1 – line for pinion and φ_2 – line for wheel. Figure 8a) presents the TCA results with non-parallelism deviation $\kappa_y = 0,008°$. As the result the locus of contact points on teeth surfaces hinge towards the tip of the pinion tooth and root of the wheel tooth while entering the meshing till half of the toothed ring. Inverse situation occurs while motion of contact point from half of the toothed ring till leaving the meshing. Then the locus of contact points on teeth surfaces is hinged towards root of pinion tooth and tip of wheel tooth. Moreover loci of contact points are not yet the φ_1 – line and φ_2 – line. It can cause change in surface pressure and sliding velocity across the width of toothed ring while in ideal gear pair these values are constant.

As results from simulations carried out for gear pair with axis misaligned error this deviation does not essentially changes the contact point motion.

Figure 8b) presents the results of tooth contact analysis of gear pair with axes distance error $\Delta a_x = 0,03$ mm. In that case real pressure angle decreases which can be observed as a translation of loci of contact points on tooth surfaces towards the root of pinion tooth and tip of wheel tooth. These lines are still the φ_1 – line for pinion and φ_2 – line for wheel.

4. Geometric contact region

Geometric contact region means the contact region obtained by the analysis of the geometry of surfaces in contact without taking into consideration elastic deformations.

One of the method of obtaining a contact pattern is a method in which a contact pattern is a set of points for which the distance between the teeth measured through the pinion tooth surface unit normal is less than the thickness of paint in a no-load contact pattern test [6]. The above-mentioned distance is represented by the length of $\bar{k}$ vector (Fig. 9).
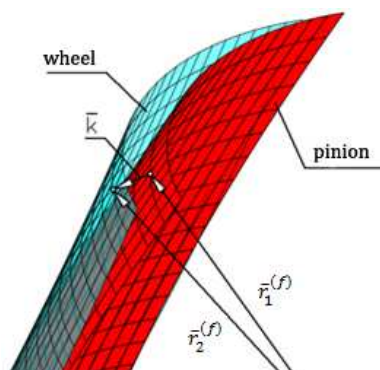

Fig. 9. Designation of distance between the teeth

For determining the length of vector $\bar{k}$ with given surface parameters θ_1 and φ_1 the system of three equations with the unknowns k, θ_2 and φ_2 specified by vector equation (21) should be solved

$$\bar{r}_1^{(f)}(\theta_1, \varphi_1) + \bar{k}(\theta_1, \varphi_1) = \bar{r}_2^{(f)}(\theta_2, \varphi_2) \tag{21}$$

where $\bar{k} = k\bar{n}_1^{(f)}$ is the length vector perpendicular to pinion tooth surface. The points for which the k value is less or equal the paint thickness are set on the $r_{M1}(b_{M1})$ graph. The r_{M1} and b_{M1} values are given by equations (22)

$$r_{M1} = \sqrt{\left(r_{x1}^{(f)}\right)^2 + \left(r_{y1}^{(f)}\right)^2}, \quad b_{M1} = r_{z1}^{(f)} \tag{22}$$

5. Influence of gears parameters on contact region

The influence of gears parameters on a contact region was investigated for gearing with data presented in Table 1.

Table 1. Data of analysed Novikov gear pair

	Pinion	Wheel
Normal module [mm]	$m_n = 3$	$m_n = 3$
Number of teeth [-]	$z_1 = 23$	$z_2 = 56$
Overlap ratio [-]	$\varepsilon_\beta = 1,2$	$\varepsilon_\beta = 1,2$
Gear width [mm]	$b = 36$	$b = 36$
Normal pressure angle [°]	$\alpha_n = 20$	$\alpha_n = 20$
Translation of convex tooth profile [mm]	$d_{CO\prime} = 0$	$d_{CO\prime} = 0$
Profile	convex	concave
Profile radius [mm]	$\rho_1 = 5,0949$	$\rho_2 = 5,2733$
Pitch diameter [mm]	$d_1 = 72,785$	$d_2 = 177,215$
Tip diameter [mm]	$d_{a1} = 79,685$	$d_{a2} = 177,215$
Root diameter [mm]	$d_{f1} = 71,285$	$d_{f2} = 169,415$

The parameter which influence on the contact region was currently analysed was change in some range along with the additional dependent parameters. Figure 10 shows contact region obtained with a method in which the distance between the teeth was measured through the unit normal.
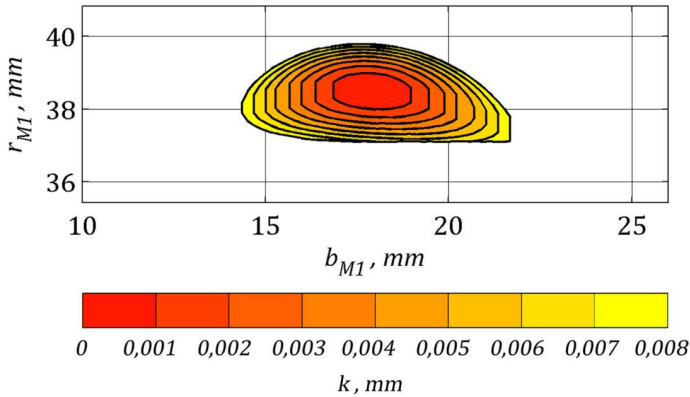
Fig. 10. Contact pattern obtained with method in which the distance
is measured through the unit normal

Colors from yellow to red represent distance from 0 to 0,008 mm.
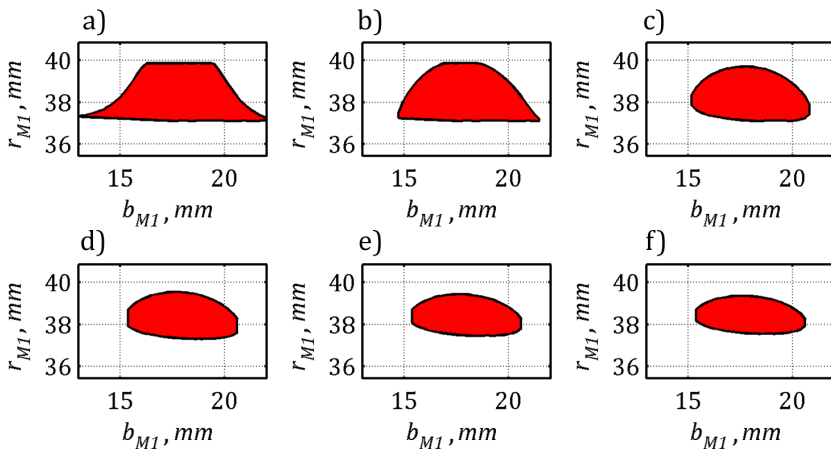The influence of ratio of teeth profiles on a contact pattern is shown in
Fig. 11.

Fig. 11. Influence of ratio of teeth profiles on a contact pattern: a) ${\rho_2}/{\rho_1} = 1{,}005$, b) ${\rho_2}/{\rho_1} = 1{,}015$, c) ${\rho_2}/{\rho_1} = 1{,}025$, d) ${\rho_2}/{\rho_1} = 1{,}035$, e) ${\rho_2}/{\rho_1} = 1{,}045$, f) ${\rho_2}/{\rho_1} = 1{,}055$

The increase of ratio of teeth profiles decreases the area of contact and it
becomes elliptical. For small values of this parameter (Fig. 11a and 11b) contact
pattern is spread all over the tooth height. It can cause stress concentration and
spalling of pinion or wheel tooth tip. However gearing with low ratio of teeth
profiles due to high level of conformity of surfaces and what follows high

contact area can be distinguished by high surface strength. In that case surface stress calculations cannot be based on the Herzt theory for three-dimensional contact problem.

Figure 12 presents the influence of ratio of pinion tooth profile radius to pinion pitch radius on a contact region.
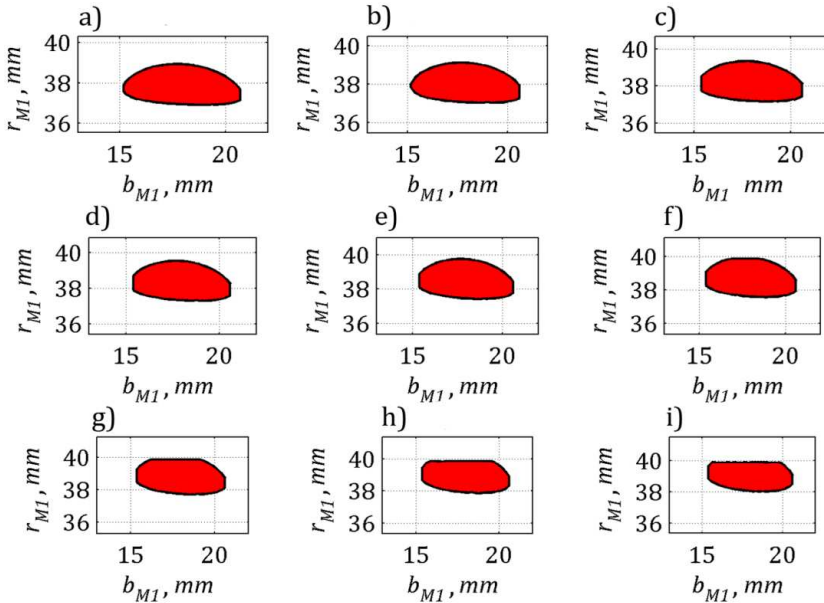

Fig. 12. Influence of ratio of pinion tooth profile radius to pinion pitch radius on a contact region: a) $\rho_1/r_1 = 0{,}11$, b) $\rho_1/r_1 = 0{,}12$, c) $\rho_1/r_1 = 0{,}13$, d) $\rho_1/r_1 = 0{,}14$, e) $\rho_1/r_1 = 0{,}15$, f) $\rho_1/r_1 = 0{,}16$, g) $\rho_1/r_1 = 0{,}17$, h) $\rho_1/r_1 = 0{,}18$, i) $\rho_1/r_1 = 0{,}19$

The increase of ratio of pinion tooth profile radius to pinion pitch radius moves the contact pattern towards the tip of the pinion tooth. It can cause the edge contact and stress concentration. Sometimes it is desirable to locate the contact pattern near the tip of pinion tooth (Fig. 12h and 12i). It can prevent the edge contact after the assembly errors occurs.

Figure 13 presents the influence of normal pressure angle on a contact region.

For small values of normal pressure angle contact region moves towards the pinion tooth root. The increase of normal pressure angle increases the contact area to maximum value for pressure angle 20°. Further increase of pressure angle decreases the contact area which becomes elliptical and moves towards tip of pinion tooth. For the same reasons which were mentioned in case of ratio of pinion tooth profile radius to pinion pitch radius it is sometimes required to locate the contact pattern near the pinion tooth as it is for 24°.
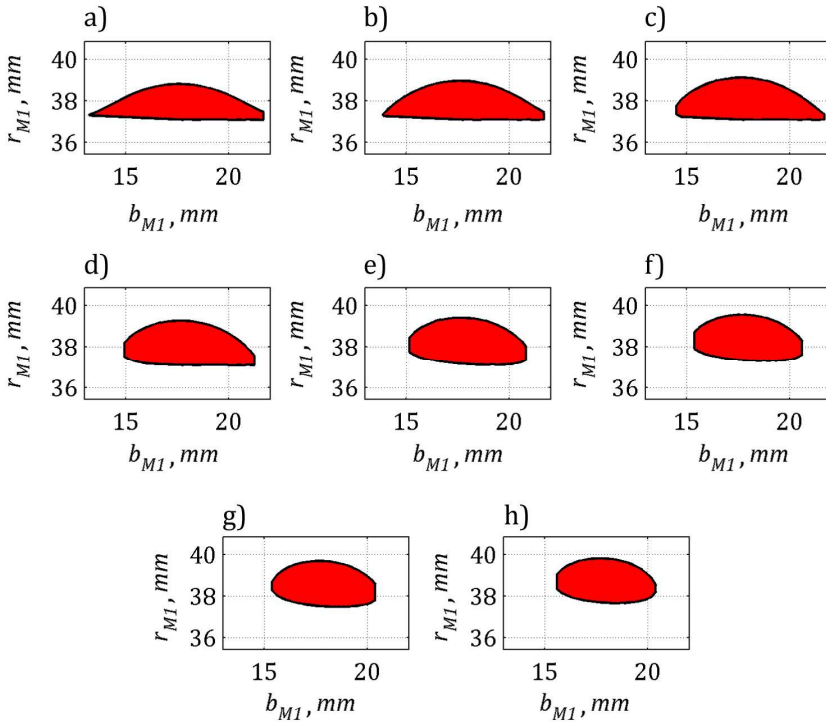
Fig. 13. Influence of normal pressure angle on a contact region: a) $\alpha_n = 10°$, b) $\alpha_n = 12°$, c) $\alpha_n = 14°$, d) $\alpha_n = 16°$, e) $\alpha_n = 18°$, f) $\alpha_n = 20°$, g) $\alpha_n = 22°$, h) $\alpha_n = 24°$

Figure 14 shows the influence of translation of convex tooth profile.

For its negative values contact pattern is a deformed ellipse, which narrows in the negative direction of axis of abscissae. For positive values deformed ellipse narrows in the positive direction. For small or high values of translation the edge contact appears.

Figure 15 presents the influence of the axes distance error on a contact region.

The increase of the axes distance error decreases the real pressure angle and therefore contact region moves through the pinion tooth root and decreases contact area. The negative influence of axes distance error can be compensate by proper location of contact pattern for ideal gearbox. Then after the assembly point of contact as well as the contact region will take the desirable position.
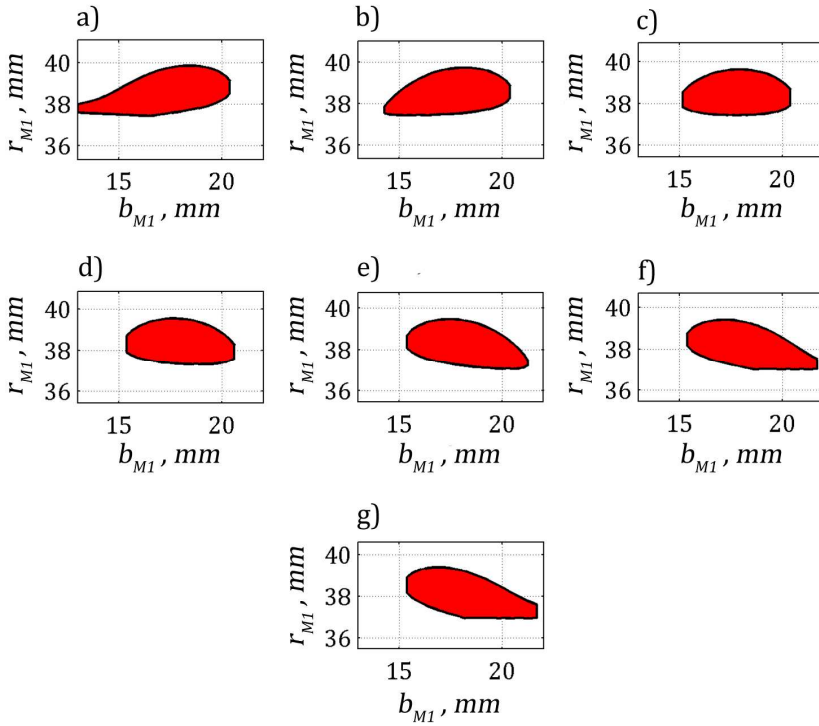
Fig. 14. Influence of translation of convex tooth profile: a) $d_{co'} = -0.6\ mm$,
b) $d_{co'} = -0.4\ mm$, c) $d_{co'} = -0.2\ mm$, d) $d_{co'} = 0\ mm$, e) $d_{co'} = 0.2\ mm$,
f) $d_{co'} = 0.4\ mm$, g) $d_{co'} = 0.6\ mm$

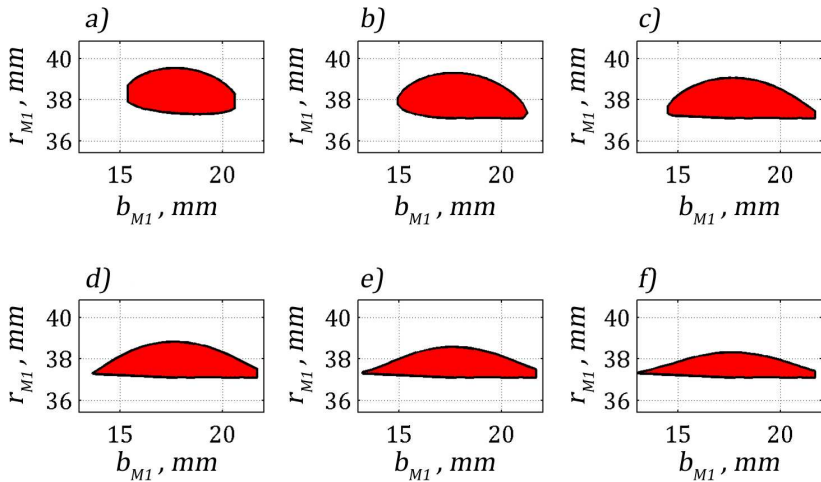Fig. 15. Influence of the axes distance error on a contact region: a) $\Delta a_x = 0$, b) $\Delta a_x = 0.01 mm$,
c) $\Delta a_x = 0.02 mm$, d) $\Delta a_x = 0.03 mm$, e) $\Delta a_x = 0.04 mm$, f) $\Delta a_x = 0.05 mm$,

Conclusions

Based on the developed mathematical model of convexo-concave Novikov gear mesh the detailed analysis of teeth contact has been performed in this paper. Knowledge of the influence of gear parameter on contact region allows to determine its optimal values which can compensate assembly errors such as misalignment and distance axes errors.

The decrease of the ratio of the radius of teeth profiles increases the area of contact and extremely increases the sensitivity of gearbox to change in axes distance. What is more if the shape of contact pattern is known it is possible to determine the boundary value of this ratio after which surface stress calculations can be performed by means of Hertz theory which assume non-conforming surfaces and elliptical contact area.

The increase of the ratio of tooth profile radius to pitch radius (or increase pressure angle) moves the contact area towards the tip of the pinion tooth.

The increase of the axes distance error decreases real pressure angle, moves contact pattern to the root of the pinion tooth and decreases the contact area. It can be compensate by proper choice of ratio of tooth profile radius to pitch radius or pressure angle.

Presented mathematical model can be also useful in the designing of tools for machining this type of gears.

References

[1] A. DYSON, H.P. EVANS, W. SNIDLE: Wildhaber-Novikov circular arc gears: Geometry and Kinematics. *Proceedings of The Royal Society A Mathematical Physical and Engineering Sciences*, **403**(1986)1825, 313-349.

[2] A. DYSON, H.P. EVANS, W. SNIDLE: Wildhaber-Novikov cicrular-arc gears: some properties of relevance to their design. *Proceedings of The Royal Society A Mathematical Physical and Engineering Sciences,* **425**(1989)1825, 341-363.

[3] D.V. ELLIS: The Westland Lynx. *The RUSI Journal*, **125**(1980)4, 70-73.

[4] S.P. RADZEVICH: Mathematical modeling of contact of two surfaces in the first order of tangency. *Mathematical and Computer Modeling*, **39**(2004)9-10, 1083-1112.

[5] P. SKAWIŃSKI, M. KRET: Mathematical model of the modified roll for spiral bevel gears milling machines. *Advances in Manufacturing Science and Technology*, **37**(2013)2, 59-71.

[6] J. WIKTOR: Analityczno-numeryczne metody analizy parametrów geometrycznych, zakłóceń ruchu i wytrzymałości przekładni walcowych. Oficyna Wydawnicza Politechniki Rzeszowskiej, Rzeszów 2004.

[7] F.L. LITVIN, A. FUENTES: Gear Geometry and Applied Theory. Cambridge University Press, Cambridge 2004.

[8] F.L. LITVIN, et al.: New version of Novikov–Wildhaber helical gears: computerized design, simulation of meshing and stress analysis. *Computer methods in applied mechanics and engineering*, **191**(2002)49-50, 5707-5740.